Near-IR Laser-Triggered Target Cell Collection Using a Carbon Nanotube-Based Cell-Cultured Substrate

Takao Sada,[†] Tsuyohiko Fujigaya,[†,*] Yasuro Niidome,[†] Kohji Nakazawa,[§,‡] and Naotoshi Nakashima[†,‡,*]

[†]Department of Applied Chemistry, Graduate School of Engineering, Kyushu University, 744 Motooka, Nishi-ku, Fukuoka 819-0395, Japan, [‡]Core Research of Evolutional Science & Technology (CREST), Japan Science and Technology Agency (JST), 5 Sanbancho, Chiyoda-ku, Tokyo 102-0075, Japan, and [§]Department of Chemical Processes and Environments, Faculty of Environmental Engineering, The University of Kitakyushu 1-1, Hibikino, Wakamatsu-ku, Kitakyushu, Fukuoka 808-0135, Japan

ABSTRACT Unique near-IR optical properties of single-walled carbon nanotube (SWNTs) are of interest in many biological applications. Here we describe the selective cell detachment and collection from an SWNT-coated cell-culture dish triggered by near-IR pulse laser irradiation. First, HeLa cells were cultured on an SWNT-coated dish prepared by a spraying of an aqueous SWNT dispersion on a glass dish. The SWNT-coated dish was found to show a good cell adhesion behavior as well as a cellular proliferation rate similar to a conventional glass dish. We discovered, by near-IR pulse laser irradiation (at the laser power over 25 mW) to the cell under optical microscopic observation, a quick single-cell detachment from the SWNT-coated surface. Shockwave generation from the irradiated SWNTs is expected to play an important role for the cell detachment. Moreover, we have succeeded in catapulting the target single cell from the cultured medium when the depth of the medium was below 150 μm and the laser power was stronger than 40 mW. The captured cell maintained its original shape. The retention of the genetic information of the cell was confirmed by the polymerase chain reaction (PCR) technique. A target single-cell collection from a culture medium under optical microscopic observation is significant in wide fields of single-cell studies in biological areas.

KEYWORDS: carbon nanotubes · single cell collection · nanotube-coated cell-cutured dish · laser pressure catapulting · near-IR pulse laser

The use of carbon nanotubes (CNTs) for biological applications has attracted considerable interest due to their unique optical, mechanical, and electrical properties together with the characteristic one-dimensional structure of the CNTs.[1] Especially, unique near-IR (NIR) laser responsive properties, such as a strong photoabsorption,[2,3] photothermal conversion,[2] and photoacoustic generation[3] due to their large π-conjugated structures have been utilized for biological applications by taking advantage of the transparency of biological tissue in the NIR region.[4] Dai *et al*. reported the pioneering work regarding the photothermal therapy[2] and photoacoustic imaging[3] of cancer *in vivo* using CNTs; since then, extensive interest has focused on this topic.[5−9] Another important aspect of CNT applications in biology is tissue engineering using CNTs as the scaffold material. The unique one-dimensional structure and hydrophobic nature of the CNTs afford acceleration of the cell growth[10−13] and provide a better cell adhesion property.[14,15]

We now describe, for the first time, the selective cell detachment and collection from a single-walled carbon nanotube (SWNT)-coated cell-culture dish triggered by NIR pulse laser irradiation. Selective separation of living cells is of interest, especially for stem cell research, organ culturing and tissue engineering.[16,17] Since conventional separation techniques, such as the aspiration of the cells using capillaries, are tedious, time-consuming, and risky due to contamination,[18,19] a simple technique realizing the selective cell detachment and collection using laser irradiation is strongly required due to the high resolution, precise positioning, and remote controllability of the laser.[20−22]

RESULTS AND DISCUSSION

Preparation of SWNT-Coated Dish and Cell Culture on SWNT-Coated Dish. In this study, a glass-bottom dish was coated by spraying an aqueous solution of the SWNTs dissolved by carboxymethylcellulose sodium salt (CMC-Na).[23] The unbound CMC-Na that remained on the SWNT-coated dish was removed by immersion in water for one day. After this procedure, the surface resistivity of the substrate reduced from 4.3×10^3 to 1.4×10^3 Ω/□ (Figure 1a), whose value was almost constant even after a subsequent two-week immersion in water, indicating a stable SWNT immobilization on the dish. A photograph of the sprayed dish shows a slightly grayish color due to a thin SWNT coating on the dish (see Supporting Information, Figure S1). The AFM image of the

* Address correspondence to fujigaya-tcm@mail.cstm.kyushu-u.ac.jp, nakashima-tcm@mail.cstm.kyushu-u.ac.jp.

Received for review December 4, 2010 and accepted May 31, 2011.

Published online May 31, 2011
10.1021/nn2012767

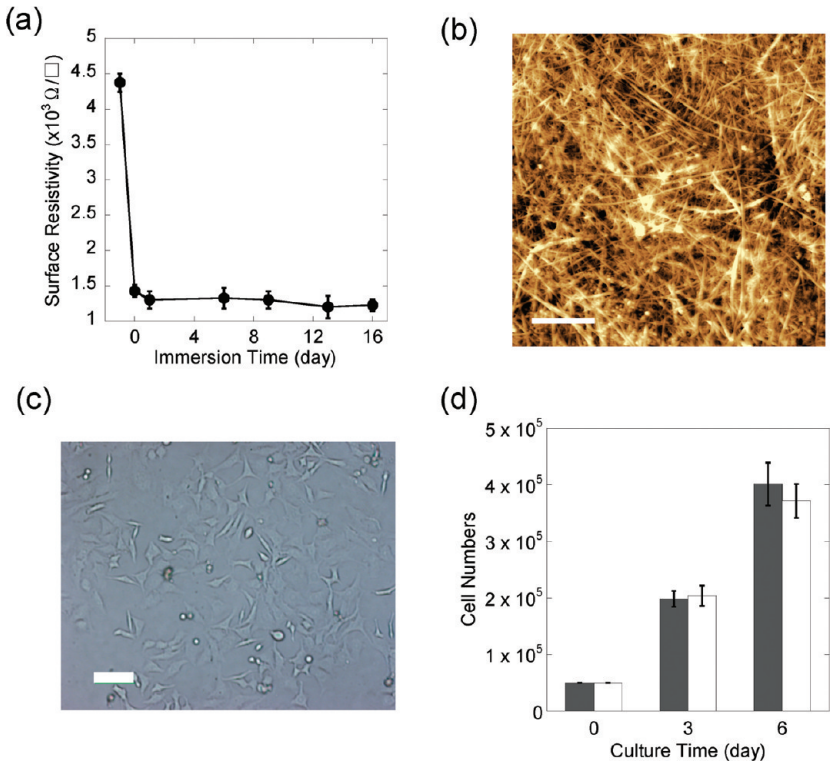

Figure 1. (a) Plots of the surface resistivity (measured in air) of the SWNT-coated dish as a function of the water immersion time. (b) AFM image of the SWNT-coated dish surface after dipping for 1 day. Scale bar: 1 μm. (c) Optical microscope image of the HeLa cells cultured on the SWNT-coated dish. Scale bar: 100 μm. (d) Comparison of the cell numbers attached to the SWNT-coated dish (black bar) and a glass dish (white bar).

SWNT-coated dish surface after the immersion and then drying is shown in Figure 1b, in which we clearly observe the SWNT network structure. The average surface roughness of the SWNT substrate determined using the AFM height profile was ~6.7 nm. The obtained SWNT-coated dish and a glass dish for comparison were used for the cell cultivation. Figure 1c shows the optical microscope image of the HeLa cells cultured on the SWNT-coated dish for 3 days. The SWNT-coated dish was found to show a similar adhesion behavior with the glass dish in terms of a cellular proliferation rate as plotted in Figure 1d and the morphology (see Supporting Information, Figure S2). For the longer culture, the cells in both dishes reached a confluent state and no difference in their stability was recognized. Such a good cytocompatibility of the CNT-coated dish was confirmed by several groups.[24] Interestingly, in some cell lines, a better cellular attachment and growth rate were reported when compared to those of a conventional culture dish due to (i) the strong interaction between the cells and fibrous CNTs[25] and (ii) higher ability of the CNTs to adsorb adhesive proteins.[26] We assumed that the growth rate of the HeLa cell was originally high and no significant difference was recognized for the SWNT-coated dish in our case.

Cell Detachment Triggered by NIR Irradiation. An NIR pulse laser (1064 nm, 4 ns) was irradiated to the cells under monitoring by an optical microscope. Interestingly, a very fast detachment of the cells in the irradiated area at a laser power over 25 mW (Figure 2a; right) was recognized, while the cell on glass dish stayed unchanged. It is evident that the detachment of the cells is derived from the SWNT-coating response to the NIR laser irradiation. This technique is applicable not only for the removal of large cell population detachments, but also for the single cell detachment by varying the focus area using different objective lenses (Figure 2b). To reveal the mechanism of the cell detachment, a blank experiment using the SWNT-coated dish in the absence of the HeLa cells was conducted. We irradiated the substrate position denoted by the letter "K" by moving the microscope stage (Figure 2c; left) and found that, by measuring the Raman mapping of the irradiated area monitored at the G-band (1590 cm^{-1}), no SWNTs remained in the letter "K" area (Figure 2c; right). The obtained result strongly suggests that the cell detachment is accompanied by the SWNT detachment triggered by the NIR pulse laser irradiation. Indeed, a change in the objective lens varies the detached area of the SWNT as clearly monitored by the optical microscope observations (Figure 2d, see also Supporting Information, Figure S3). This result suggests that the controllability of the cell detachment as shown in Figure 2a,b is associated with the SWNT detachment.

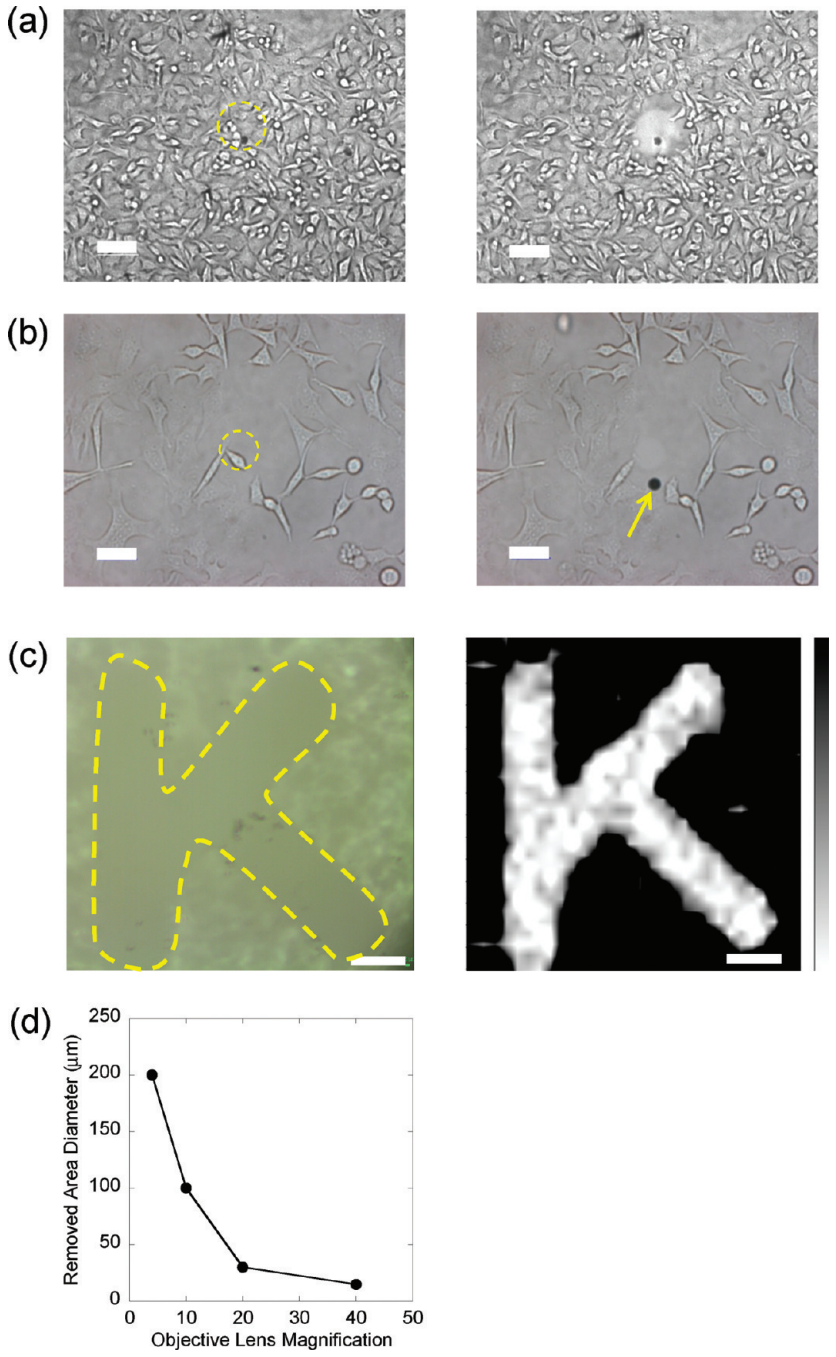

Figure 2. (a) Optical microscopic images of the HeLa cells on the SWNT-coated dishes before (left) and after (right) the NIR pulse irradiation at a power of 40 mW through a 10× objective lens. The focused area is indicated by the yellow circles. Scale bars, 100 μm. (b) Microscopic images of the HeLa cells on the SWNT-coated dish before (left) and after (right) the NIR pulse irradiation at a power of 25 mW using a 20× objective lens. The focused area is indicated by a yellow circle. The yellow allow indicates the bubble generated after the NIR irradiation. Scale bars: 50 μm. (c) Optical microscopic image (left) and Raman mapping monitored by G-band peak (right) of SWNT-coated dish after NIR irradiation. The NIR laser was irradiated in the shape of a "K" as indicated by the yellow line. Scale bars: 25 μm. (d) Plots of the removed area as a function of the objective lens magnification.

The effects of the NIR pulse laser irradiation for SWNTs have been investigated by several groups, and the general understanding for the irradiation is the induction of an effective photoacoustic effect.[27−29] The intense photoacoustic response of the SWNTs generates a shockwave around a surrounding medium, which sometime causes bubble formation as well as transformation of the SWNTs into different types of various carbons.[27−29] In our case, the generation of the shockwave was evidenced by the bubble formation (Figure 2b; indicated by arrow). It was assumed that the shockwave generation from the irradiated SWNTs resulted in the cell detachment.

Cell Catapulting Triggered by NIR Irradiation. Quite interestingly, we found that the detached cells were

catapulted from the cultured medium when the depth of the cultured medium was less than 150 μm and the irradiated laser power was ~40 mW as shown in Figure 3a. In Figure 3b, the snapshots of the cultured medium surface monitored using a high speed camera during the NIR laser irradiation is shown, from which we found that the generation of ripples, and at the same time, the cell catapulted from the substrate surface (Figure 3b; indicated by arrow). The snapshot image analysis allows us to calculate the flying rate of the cell in air to be as fast as 1.25 m/s.

The optical microscopic image of the substrate placed 10 mm above the medium surface during several pulse shots is shown in Figure 4a (left). Several objects whose sizes are similar to those of the HeLa cells (10−20 μm) were observed on the substrate. The fluorescence image of the same area (Figure 4a; right) staining with a mixture of Calcein-AM and PI shows a clear red fluorescence due to the intercalation of the PI into the double-stranded DNA, indicating that the observed images are HeLa cells captured on the substrate. The absence of green fluorescence of Calcein-AM and the presence of red fluorescence from PI imply the termination of the cell activity.

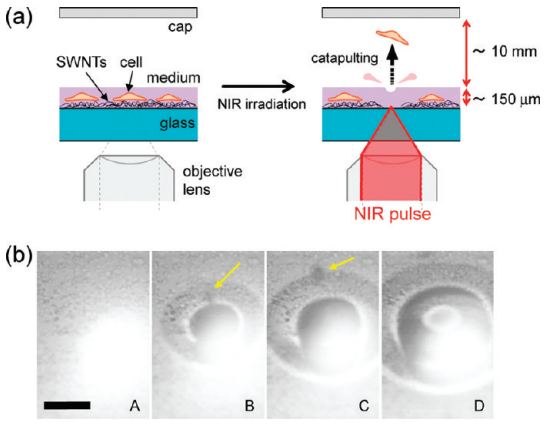

Figure 3. (a) Schematic illustration of NIR catapulting of the cell. (b) Snapshots of the surface of cultured medium monitored by a high speed camera at 0 (A), 0.1 (B), 0.2 (C), and 0.3 (D) ms after NIR irradiation. The catapulted cell is marked by the yellow arrow. Scale bar: 0.25 mm.

It is worth mentioning that the present technique allows us to collect the cells without any fragmentation even in the absence of supporting materials.[30] In the conventional UV laser pressure catapulting (LPC) technique, a thick UV absorbing film (~1.35 μm)[31] used for the pulse absorber supports the shape of the cells during catapulting. However, the thick films make optical microscopic observations of the catapulted cells difficult when the films under of the cell come to the front side of the cells after catpulting.[30] On the other hand, the effective energy conversion of the SWNTs requires only small amounts of the SWNT layer (~40 nm in thickness) for catapulting, enabling the further analysis of the catapulted cells using the microscope observation such as the fluorescent measurement describing above.

We also carried out scanning electron microscope (SEM) measurements of the catapulted cell. As shown in Figure 4b (right), it was clear that by comparison to the cell before the catapulting as shown in Figure 4b (left), no cell fragmentation occurred and the cell morphology was retained. Such a microscopic observation will offer useful information in order to analyze the structural as well as functional properties of the cells of interest.

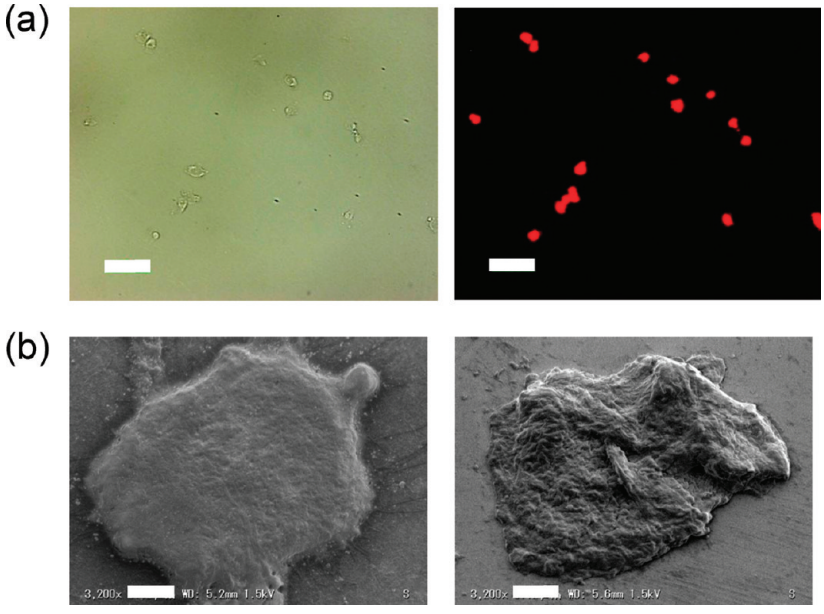

Figure 4. (a) Optical microscope image of the catapulted cells (left) and the fluorescent microscope image in the same area (right). Scale bars: 100 μm. (b) SEM images of the HeLa cell on the SWNTs dish measured after the removal of the culture medium (left; scale bar = 5 μm) and the catapulted cell on silicon substrate (right; scale bar = 5 μm).

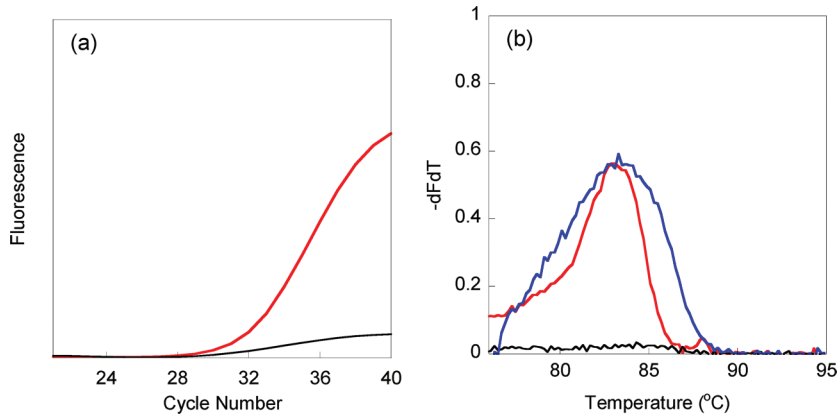

Figure 5. (a) Monitoring the fluorescence on the PCR cycles in the presence (red line) and absence (black line) of the catapulted cell. (b) The melting curves of the PCR products measured using the captured single cell (red line) and 350 collected cells from the culture dish (blue line). The black line shows the result of the blank test for a sample not containing the cell.

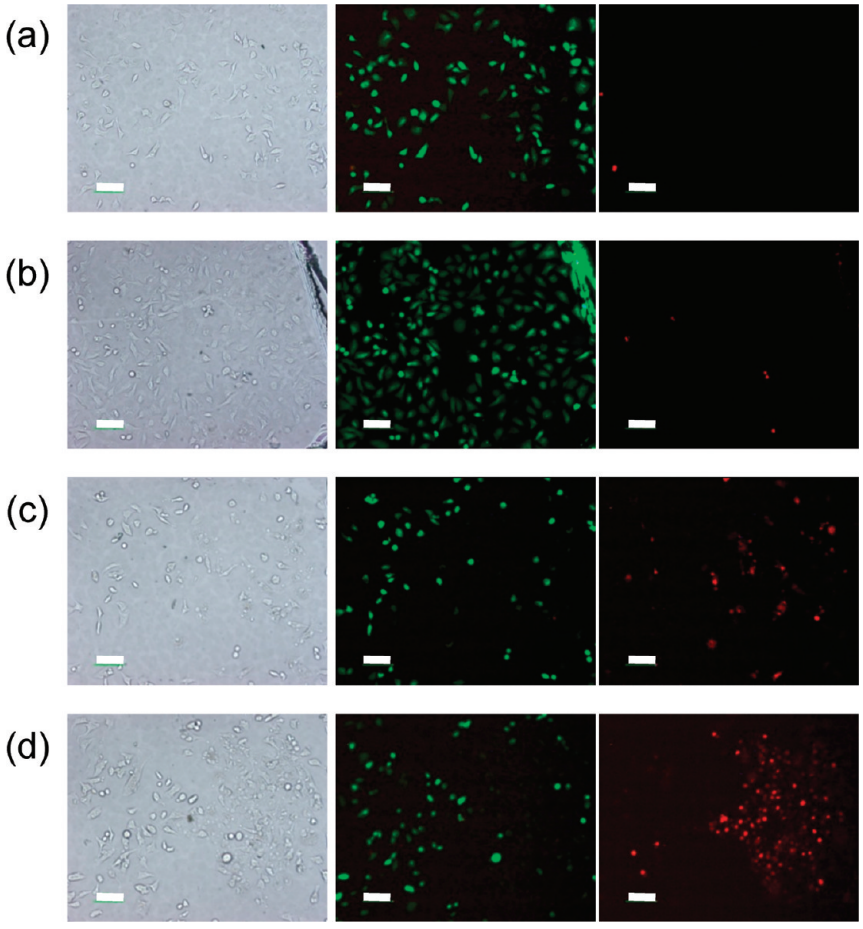

Figure 6. Optical microscope (left), Calcein-AM fluorescent (middle), and PI fluorescent (right) images at 2 (A), 4 (B), 6 (C), and 8 mW (D) irradiation. Scale bars: 100 μm.

Gene Analysis of the Catapulted Cell. As a functional analysis for the catapulted single cell, we carried out an RNA analysis using the real-time reverse transcription polymerase chain reaction (RT-PCR) technique. The glyceraldehyde-3-phosphate dehydrogenase gene (GAPDH), a typical housekeeping gene for the translation of the dehydrogenase protein, was chosen as the target because the HeLa cell contains the sequence. Figure 5a (red line) shows the amplification plot monitoring of the RT-PCR using the GAPDH primer and the complement DNA (cDNA) of the RNA obtained from the captured single cell (see Method section). We observed an increase in the fluorescent intensity corresponding to the gene amplification. Based on the

control experiment carried out in the absence of the catapulted cell that shows a very weak fluorescent in Figure 5a (black line), it is obvious that the signal originated from the genetic information of the catapulted single cell. The sharp and unimodal melting profile of the amplified gene indicates that the genes are a single component (Figure 5b, red line). The profile for the captured single cell almost coincided with that of the 350 cells collected from the culture dish (Figure 5b, blue line). Such a peak is not observed in the absence of the cell (Figure 5b, black line). All the obtained results clearly state that the amplified gene originated from the GAPDH gene in the captured single cell. Now it is evident that the catapulted cell retains the genetic information. It is worth emphasizing that a functional analysis using the captured single cell is possible. The present technology would provide a novel tool for cell bioengineering.

Evaluation of Cell Viability. To address the effect of the NIR laser power for the cell viability, we carried out a series of fluorescent staining studies for samples obtained after different power laser irradiations. Figure 6 shows the optical and fluorescent microscope images of the HeLa cells cultured on the SWNT surface after the NIR irradiation of only the right half area of the images. The images were taken 10 min after the irradiation. It is clear that the green fluorescence was dominant when the irradiation power was less than 4 mW, and the red fluorescent spots increased when the NIR power was greater than 6 mW. The results obviously indicate that the NIR laser causes termination of the cell activity and the termination occurs below the power of cell removal (~25 mW). The temperature thresholds leading to cell death are high for a short power exposure time.[31] For example, Simanovskii *et al*. estimated that the cell survivable temperature could be as high as 130 °C for a 300 μs exposure by a CO_2 laser at the wavelength of 10600 nm.[32] Assuming that all the energy absorbed by the irradiated SWNTs is converted to heat, the temperature change at the irradiated SWNT interfaces is roughly calculated to be 2300 °C/pulse cm^2 (see Supporting Information). Because the irradiation time for our system is quite short (4 ns) and the cells are placed on the adhesive proteins on the SWNT coating, the direct effect of the pulse heating of the SWNTs on the cell termination is rather difficult to estimate. At this moment, we assumed that the mechanism of the cell termination is due to the disordering of the cell membrane triggered by the shockwave since the PI molecules can only penetrate into the damaged membrane.[33,34] Similarly, it is explained that the termination of the cell activity observed for the cell catapulting experiments carried out at a higher power, 40 mW as displayed in Figure 4a, was also induced during the laser irradiation. Although some cell analyses, such as the proliferating ability of the catapulted cells, are limited, the present technique is useful for subsequent genomic or proteomic analyses as demonstrated in Figure 5.

CONCLUSIONS

The selective detachment of the cells is achieved by the NIR irradiation of the cells cultured on a SWNT-coated dish. The shockwave generated by the NIR pulse laser irradiation of the SWNTs plays an important role in the detachment of the cell. By increasing the laser power as well as decreasing the depth of the cultured medium, the detached cells are readily catapulted onto the substrate placed close to the medium surface. Such a catapulting method enables the highly selective collection of the targeted cells of interest and is a very useful tool for single cell studies. The SEM experiment revealed that no fragmentation occurred for the catapulted cell. The RT-PCR analysis for the catapulted single cell revealed the retention of the genetic information. The light-induced cell detachment technique would be also applicable as a novel cell patterning technique, and such studies are currently underway in our laboratories.

METHODS

Materials. The SWNTs (synthesized by an arc method) were purchased from Meijo Nano Carbon. Carboxymethyl cellulose sodium salt (CMC−Na) was purchased from Kishida Cemical and used as received.

Fabrication of an SWNT-Coated Dish. CMC-Na (3 mg) and the SWNTs (1 mg) were dissolved in H_2O (10 mL) by sonication using a bath-type sonicator (Branson 5510) for 120 min, followed by centrifugation (10000*g*) using a ultracentrifugator (Kubota, 3K30C) for 15 min. The obtained SWNT aqueous dispersion was sprayed on a glass substrate (Glass Base Dish, IWAKI, 27 mm φ) placed on a temperature-controlled sheet at 100 °C. The obtained SWNT-coated dish was immersed in deionized water and dried with flowing N_2 gas. For the cell culture, the dish was sterilized by ultraviolet radiation for 24 h.

Cell Culture. The HeLa cells were seeded on the SWNT-coated dish. The cells were cultured in D-MEM (Wako) with 10% FBS and antibiotic-antimycotic (GIBCO) at 37 °C in humidified 5% CO_2.

Measurements. An atomic force microscope (AFM) study was conducted using a probe microscope (SHIMADZU, SPM-9600). The surface resistivity measurements were performed using a resistivity meter (Mitsubishi Chemical Analytech, MCP-T600). The SEM observations were carried out using a digital SEM (Keyence Co., VE-9800).

Selective Detachment. The HeLa cells cultured SWNT-coated dish was placed on the stage of an inverted microscope (Nikon, TE2000) equipped with a stage-top incubator (Tokai Hit, ONICS). A near-infrared (NIR) laser beam from a pulse laser (Nd: YVO_4, 1064 nm, 20 Hz; New Wave Research, Polaris III) with a pulse duration of 4 ns was focused on the SWNT-coated dish through the objective lens (4×, NA = 0.13; 10×, NA = 0.3; 20×, NA = 0.45; 40×, NA = 0.6). The microscope images were monitored by a CCD video camera (Watec, model WAT-221S). The actual laser power was monitored by an energy meter

display (Ophir Optronics, Orion TH) equipped with a thermal head (Ophir Optronics, 30A-P). The cell catapulting was monitored by a high speed camera (IDT Japan, MOTION Pro Y4S-2).

Real-Time RT-PCR of Catapulted Cell. One of the cells cultured on the SWNT-coated dish was catapulted to the cap of the PCR tube by the NIR irradiation. Cell lyses buffer (20 μL, Ambion, Cells-to-cDNA II kit) was added to the cap of the PCR tube and the cell was collected in the PCR tube. The obtained cell lysis solution was heated at 75 °C for 10 min to inactivate the RNases in the cells and incubated at 5 °C for 5 min. The DNase I solution (Ambion, Cells-to-cDNA II kit) in sterilized water (1 μL, 0.4 μL/μL) was added to the cell lysis solution and incubated at 37 °C for 15 min to degrade the genomic DNA. To inactivate the DNase, the solution was heated at 75 °C for 5 min. For the reverse transcription, the mixture of the cell lysis solution (10 μL), dNTP Mix (4 μL, Ambion, Cells-to-cDNA II kit) and oligo (dT) primers (2 μL, Ambion, Cells-to-cDNA II kit) in the PCR tube was heated at 70 °C for 3 min and incubated at 5 °C for 1 min. Room temperature buffer (10×, 2 μL, Ambion, Cells-to-cDNA II kit), M-MLV Reverse Transcriptase (1 μL, Ambion, Cells-to-cDNA II kit) and RNase Inhibitor (1 μL, Ambion, Cells-to-cDNA II kit) were added to the solution and incubated at 42 °C for 60 min, then at 92 °C for 10 min to provide a cDNA solution transcribed from the RNA of the captured cells. For the PCR, the cDNA solution (5 μL), 10× PCR buffer (5 μL), dNTP Mix (4 μL, Ambion, Cells-to-cDNA II kit), human GAPDH primer (2 μL, Takara, Human Housekeeping Gene primer Set), thermostable DNA polymerase (0.4 μL, Ambion, SuperTaq Plus DNA Polymerase), SYBR Green (1 μL, Takara, SYBR Green I Nucleic Acid Gel Stain) and sterilized water (30 μL) were mixed in a PCR tube. The PCR cycle (95 °C for 30 s to denature, 95 °C for 5 s for amplification, then at 60 °C for 30 s) was repeated for 40 cycles using a thermocycler (Bio Rad, PC808) equipped with a Mini Opticon (Bio Rad). The control experiment using 350 collected cells from the culture dish by a trypsin treatment was carried out in a similar fashion, in which 35 PCR cycles were repeated.

Cell Viability after NIR Irradiation. The cell viability after the NIR irradiation was estimated using a mixture of calcein-AM and propidium iodide (PI) as the fluorescent probes (DOJINDO, Cellstain Double Staining Kit). The stock solution for the mixture of calcein-AM and PI was prepared by adding 10 μL of a 1 mmol/mL calcein-AM stock solution and 15 μL of a 1.5 mmol/mL PI solution to 5 mL of Dulbecco's phosphate buffered saline (DPBS) (GIBCO). The calcein-AM/PI mixture solution in DPBS was added to the HeLa cells cultured on the SWNT-coated dish after the NIR laser irradiation through the objective lens (10×, NA = 0.3) at the powers of 2, 4, 6, and 8 mW. The cells were analyzed using a microscope (Nikon, TE2000) equipped with a filter system (G-2A excitation filter, 510−560 nm; and B-2A excitation filter, 450−490 nm).

Acknowledgment. This work was supported by the Global COE Program "Science for Future Molecular Systems" and Nanotechnology Network Project (Kyushu-area Nanotechnology Network) from the Ministry of Education, Culture, Sports, Science and Technology, Japan. The authors thank Dr. M. Kitaoka and Prof. N. Kamiya of Kyushu University for their technical assistance for the RT-PCR experiments and helpful discussion.

Supporting Information Available: Photograph and optical microscope images of the SWNT-coated dish and estimation procedure of temperature increasing triggered by NIR irradiation of SWNT coating. This material is available free of charge *via* the Internet at http://pubs.acs.org.

REFERENCES AND NOTES

1. Liu, Z.; Tabakman, S.; Welsher, K.; Dai, H. Carbon Nanotubes in Biology and Medicine: *In Vitro* and *in Vivo* Detection, Imaging and Drug Delivery. *Nano Res.* **2009**, *2*, 85–120.
2. Kam, N. W. S.; O'Connell, M.; Wisdom, J. A.; Dai, H. Carbon Nanotubes as Multifunctional Biological Transporters and Near-Infrared Agents for Selective Cancer Cell Destruction. *Proc. Natl. Acad. Sci. U.S.A.* **2005**, *102*, 11600–11605.
3. De La Zerda, A.; Zavaleta, C.; Keren, S.; Vaithilingam, S.; Bodapati, S.; Liu, Z.; Levi, J.; Smith, B. R.; Ma, T.-J.; Oralkan, O.; *et al.* Carbon Nanotubes as Photoacoustic Molecular Imaging Agents in Living Mice. *Nat. Nanotechnol.* **2008**, *3*, 557–562.
4. Weissleder, R. A Clearer Vision for *in Vivo* Imaging. *Nat. Biotechnol.* **2001**, *19*, 316–317.
5. Moon, H. K.; Lee, S. H.; Choi, H. C. *In Vivo* Near-Infrared Mediated Tumor Destruction by Photothermal Effect of Carbon Nanotubes. *ACS Nano* **2009**, *3*, 3707–3713.
6. Chakravarty, P.; Marches, R.; Zimmerman, N. S.; Swafford, A. D. E.; Bajaj, P.; Musselman, I. H.; Pantano, P.; Draper, R. K.; Vitetta, E. S. Thermal Ablation of Tumor Cells with Antibody-Functionalized Single-Walled Carbon Nanotubes. *Proc. Natl. Acad. Sci. U.S.A.* **2008**, *105*, 8697–8702.
7. Ghosh, S.; Dutta, S.; Gomes, E.; Carroll, D.; D'Agostino, R.; Olson, J.; Guthold, M.; Gmeiner, W. H. Increased Heating Efficiency and Selective Thermal Ablation of Malignant Tissue with DNA-Encased Multiwalled Carbon Nanotubes. *ACS Nano* **2009**, *3*, 2667–2673.
8. Kim, J.-W.; Shashkov, E. V.; Galanzha, E. I.; Kotagiri, N.; Zharov, V. P. Photothermal Antimicrobial Nanotherapy and Nanodiagnostics with Self-Assembling Carbon Nanotube Clusters. *Lasers Surg. Med.* **2007**, *39*, 622–634.
9. Kang, B.; Yu, D.; Dai, Y.; Chang, S.; Chen, D.; Ding, Y. Cancer-Cell Targeting and Photoacoustic Therapy Using Carbon Nanotubes as "Bomb" Agents. *Small* **2009**, *5*, 1292–1301.
10. Hu, H.; Ni, Y.; Montana, V.; Haddon, R. C.; Parpura, V. Chemically Functionalized Carbon Nanotubes as Substrates for Neuronal Growth. *Nano Lett.* **2004**, *4*, 507–511.
11. Kalbacova, M.; Kalbac, M.; Dunsch, L.; Kataura, H.; Hempel, U. The Study of the Interaction of Human Mesenchymal Stem Cells and Monocytes/Macrophages with Single-Walled Carbon Nanotube Films. *Phys. Status Solidi B* **2006**, *243*, 3514–3518.
12. Zanello, L. P.; Zhao, B.; Hu, H.; Haddon, R. C. Bone Cell Proliferation on Carbon Nanotubes. *Nano Lett.* **2006**, *6*, 562–567.
13. Tutak, W.; Park, K. H.; Vasilov, A.; Starovoytov, V.; Fanchini, G.; Cai, S.-Q.; Partridge, N. C.; Sesti, F.; Chhowalla, M. Toxicity Induced Enhanced Extracellular Matrix Production in Osteoblastic Cells Cultured on Single-Walled Carbon Nanotube Networks. *Nanotechnology* **2009**, *20*, 255101.
14. Akasaka, T.; Yokoyama, A.; Matsuoka, M.; Hashimoto, T.; Abe, S.; Uo, M.; Watari, F. Adhesion of Human Osteoblast-Like Cells (Saos-2) to Carbon Nanotube Sheets. *Biomed. Mater. Eng.* **2009**, *19*, 147–153.
15. Aoki, N.; Yokoyama, A.; Nodasaka, Y.; Akasaka, T.; Uo, M.; Sato, Y.; Tohji, K.; Watari, F. Cell Culture on a Carbon Nanotube Scaffold. *J. Biomed. Nanotechnol.* **2005**, *1*, 402–405.
16. Day, R. C.; Grossniklaus, U.; Macknight, R. C. Be More Specific! Laser-Assisted Microdissection of Plant Cells. *Trends Plant Sci.* **2005**, *10*, 397–406.
17. Meyers, B. C.; Galbraith, D. W.; Nelson, T.; Agrawal, V. Methods for Transcriptional Profiling in Plants. Be Fruitful and Replicate. *Plant Physiol.* **2004**, *135*, 637–652.
18. Brandt, S.; Kloska, S.; Altmann, T.; Kehr, J. Using Array Hybridization to Monitor Gene Expression at the Single Cell Level. *J. Exp. Bot.* **2002**, *53*, 2315–2323.
19. Wang, Z.; Potter, R. H.; Jones, M. G. K. Differential Display Analysis of Gene Expression in the Cytoplasm of Giant Cells Induced in Tomato Roots by Meloidogyne Javanica. *Mol. Plant Pathol.* **2003**, *4*, 361–371.
20. Kehr, J. Single Cell Technology. *Curr. Opin. Plant Biol.* **2003**, *6*, 617–621.
21. Thalhammer, S.; Lahr, G.; Clement-Sengewald, A.; Heckl, W. M.; Burgemeister, R.; Schutze, K. Laser Microtools in Cell Biology and Molecular Medicine. *Laser Phys.* **2003**, *13*, 681–691.
22. Eltoum, I. A.; Siegal, G. P.; Frost, A. R. Microdissection of Histologic Sections: Past, Present, and Future. *Adv. Anat. Pathol.* **2002**, *9*, 316–322.
23. Minami, N.; Kim, Y.; Miyashita, K.; Kazaoui, S.; Nalini, B. Cellulose Derivatives as Excellent Dispersants for Single-Wall Carbon Nanotubes as Demonstrated by Absorption and Photoluminescence Spectroscopy. *Appl. Phys. Lett.* **2006**, *88*, 093123/1–093123/3.

24. Li, X.; Fan, Y.; Watari, F. Current Investigations into Carbon Nanotubes for Biomedical Application. *Biomed. Mater.* **2010**, *5*, 1–12.
25. Terada, M.; Abe, S.; Akasaka, T.; Uo, M.; Kitagawa, Y.; Watari, F. Development of a Multiwalled Carbon Nanotube Coated Collagen Dish. *Dent. Mater. J.* **2009**, *28*, 82–88.
26. Li, X.; Gao, H.; Uo, M.; Sato, Y.; Akasaka, T.; Feng, Q.; Cui, F.; Liu, X.; Watari, F. Effect of Carbon Nanotubes on Cellular Functions *in Vitro*. *J. Biomed. Mater. Res. A* **2009**, *91*, 132–139.
27. Kang, B.; Dai, Y.; Chang, S.; Chen, D. Explosion of Single-Walled Carbon Nanotubes in Suspension Induced by a Large Photoacoustic Effect. *Carbon* **2008**, *46*, 978–981.
28. Kichambare, P. D.; Chen, L. C.; Wang, C. T.; Ma, K. J.; Wu, C. T.; Chen, K. H. Laser Irradiation of Carbon Nanotubes. *Mater. Chem. Phys.* **2001**, *72*, 218–222.
29. Tseng, S. H.; Tai, N. H.; Hsu, W. K.; Chen, L. J.; Wang, J. H.; Chiu, C. C.; Lee, C. Y.; Chou, L. J.; Leou, K. C. Ignition of Carbon Nanotubes Using a Photoflash. *Carbon* **2007**, *45*, 958–964.
30. Vogel, A.; Venugopalan, V. Mechanisms of Pulsed Laser Ablation of Biological Tissues. *Chem. Rev.* **2003**, *103*, 577–644.
31. Vogel, A.; Lorenz, K.; Horneffer, V.; Huttmann, G.; von Smolinski, D.; Gebert, A. Mechanisms of Laser-Induced Dissection and Transport of Histologic Specimens. *Biophys. J.* **2007**, *93*, 4481–4500.
32. Simanovskii, D. M.; Mackanos, M. A.; Irani, A. R.; O'Connell-Rodwell, C. E.; Contag, C. H.; Schwettman, H. A.; Palanker, D. V. Cellular Tolerance to Pulsed Hyperthermia. *Phys. Rev. E* **2006**, *74*, 011915.
33. Kaneshiro, E. S.; Wyder, M. A.; Wu, Y.-P.; Cushion, M. T. Reliability of Calcein Acetoxy Methyl Ester and Ethidium Homodimer or Propidium Iodide for Viability Assessment of Microbes. *J. Microbiol. Methods* **1993**, *17*, 1–16.
34. Ankarcrona, M.; Dypbukt, J. M.; Bonfoco, E.; Zhivotovsky, B.; Orrenius, S.; Lipton, S. A.; Nicotera, P. Glutamate-Induced Neuronal Death: A Succession of Necrosis or Apoptosis Depending on Mitochondrial Function. *Neuron* **1995**, *15*, 961–973.